$M_s : m_b$ RELATIONSHIPS FOR SMALL MAGNITUDE EVENTS: OBSERVATIONS AND PHYSICAL BASIS FOR m_b BASED ON REGIONAL PHASES

Howard J. Patton
Los Alamos National Laboratory

ABSTRACT

To address the challenge of small event monitoring for the Comprehensive Nuclear-Test-Ban Treaty (CTBT), there is great interest to extend the successful teleseismic m_b-M_s discriminant to regional-distance applications. Among the outstanding issues are (1) how well can we expect the discriminant to perform for regional data as a function of source size and (2) what is the physical basis behind its performance. In a recent paper Patton (2000), M_w: m_b scaling relationships for Pn and Lg waves with 1-s periods were developed for earthquakes and explosions located in distinct tectonic regions and geologic materials around the world. Among a number of findings of that study is the result that m_b(Pn) for explosions scales at a significantly higher rate than m_b(Lg) in the M_w range ~3.5 - 6.0. On the other hand, Pn and Lg scaling rates do not differ for earthquakes. On plots of M_s versus m_b(Pn), the scaling results suggest that earthquake and explosion populations converge at M_s ~ 1 -2, while populations may or may not converge on plots of M_s versus m_b(Lg), and show better separation at small magnitudes. Observations of regional M_s for small-yield explosions at the Nevada Test Site (NTS) confirm the scaling predictions. Thus, m_b based on regional shear phases may serve as a better m_b-M_s discriminant than m_b based on regional compressional phases, a surprising conclusion. These findings certainly cannot be explained by simple theories of the explosion source, and I propose a physical model combining well-established scaling models and the latest understanding of Lg generation by underground nuclear explosions.

Key Words: discrimination, regional monitoring, physical basis, regional phases

OBJECTIVE

The objective of this project is (1) to characterize m_b-M_s scaling for earthquakes and explosions using regional-distance observations and (2) to provide a physical basis for the scaling and for discrimination performance at small magnitudes. One of the greatest challenges of monitoring a CTBT is discriminating man-made seismic events from natural events at low source strengths, and this project seeks an understanding of the potential at small magnitudes using extensions of the m_b-M_s discriminant to regional data.

RESEARCH ACCOMPLISHED

A recent study of regional scaling relations found that m_b(Pn) scales at a higher rate than m_b(Lg) on plots of M_w versus m_b for explosions detonated at NTS (Patton, 2000). Scaling relations for explosions at Semipalatinsk and other hard-rock test sites suggested similar differences between Pn and Lg scaling rates, but the data sets were smaller and showed more scatter than NTS observations, and as a result, estimates of scaling rates were less certain. In contrast to explosions, earthquakes did not show differences in scaling rates for Pn and

Lg waves. In this paper, I provide further evidence that source scaling of 1-Hz Pn and Lg waves is different for NTS explosions, and I propose a physical model to explain why this might be. The verification significance of this work relates to characterization of m_b-M_s scaling and to the discrimination potential at small magnitudes. This characterization is the subject of current research, but some tentative results will be examined.

Both m_b(Pn) and m_b(Lg) were measured for most explosions conducted at NTS in order to develop better technologies for estimating seismic yield (e.g., Nuttli, 1986; Patton, 1988; Vergino and Mensing, 1990). Of special interest to this project is the frequently overlooked fact that yield-scaling reported for Lg and Pn waves differed for explosions detonated in tuff, as summarized in the table below.

Table 1: Yield-scaling results for NTS explosions (after Patton; Vergino and Mensing)

Phase	Test Region	Intercept	Yield Slope	Gas Porosity Slope
Lg	Yucca, AWT	3.52	0.96*	–
Lg	Yucca, AWT	4.13	0.75	−0.025
Lg	Yucca & Pahute, BWT	4.18	0.76*	–
Pn	So. Yucca, AWT & BWT	3.84	0.91	−0.027
Pn	Pahute, AWT & BWT	3.87	0.91	−0.027

* Yield slope when gas porosity is left out of the regression model.

Patton (1988) found that after accounting for the effects of gas porosity, yield scaling of 1-Hz Lg waves for explosions above the water table (AWT) is the same as it is for explosions below the water table (BWT). The same effect of gas porosity is seen for Pn waves (Vergino and Mensing), but the slope on log yield, 0.91, is significantly greater than it is for Lg waves, 0.76. Thus, Pn scaling rates with official yield are 20% higher than they are for Lg waves. For comparison, estimates of scaling slopes on plots of M_w versus m_b for NTS explosions are 1.37 ± 0.03 and 1.22 ± 0.03 for Pn and Lg waves, respectively (Patton, 2000), a 12% difference.

Direct comparisons of m_b(Pn) and m_b(Lg) should also reveal differences in scaling for NTS explosions. Figure 1 shows such a plot for 243 explosions ranging ~3 orders of magnitude in yield. A linear regression yields a slope of 1.13 ± 0.02. In other words, m_b(Pn) scales at a rate 13% higher than Lg waves. This estimate is about the same percentage as the one obtained from M_w versus m_b data, which used explosions detonated in a variety of media, just as Figure 1 does. The yield-scaling results in Table 1 pertain just to explosions fired in tuff and rhyolite. In any case, summarizing for NTS explosions, scaling rates are not the same for regional phases based on compressional (Pn) and shear wave (Lg) phases, as various scaling relationships reveal that rates for Pn are ~13 to 20% higher than they are for Lg.
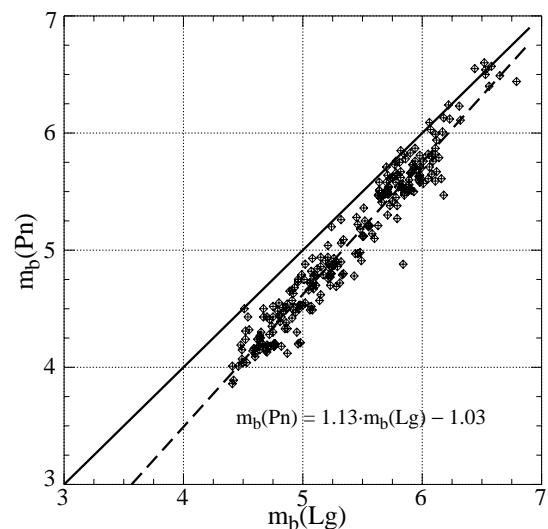

Figure 1. Regional m_b for NTS explosions. Dash line is a regression fit to the data; solid line represents equality.

A Physical Model. In this sub-section, a model combining the basic tenets of the Mueller-Murphy model (Mueller and Murphy, 1971; M-M) with recent insights into Lg generation by underground explosions is proposed to explain the differences in source scaling between Pn and Lg waves. In this development, I use the concept of an "effective" source function. An effective source function combines the features of a traditional source function with the effects of complex wave propagation on seismic wave generation. In this case, the propagation effects occur so close to the source that it is impossible to separate them in far-field data from intrinsic source properties. An example of such propagation effects is near-field Rg-to-S scattering. Gupta *et al*. (1992) proposed that this scattering mechanism is particularly effective for generating low-frequency crustal S waves (< 2 Hz) by explosions because of their shallow depth of burial and efficient Rg excitation characteristics. Subsequent research, both observational (Patton and Taylor, 1995; Gupta *et al*., 1997; Myers *et al*., 1999) and synthetic (e.g., Jih, 1993; 1995), has supported this proposed mechanism. The model of Rg-to-S scattering has undergone some refinements with subsequent research. In particular, excitation nulls observed in spectral amplitudes of Lg waves (Patton and Taylor, 1995; Gupta *et al*., 1997) were interpreted to be caused by the imprint of Rg source spectra excited by a compensated linear vector dipole (CLVD). These nulls are related to focal depth of the CLVD source, which is a kinematic description of spall phenomena occurring in the geologic strata over the explosion point source. Thus, while the explosion source is an efficient source of Rg waves, spallation, which reaches to the free surface and has a centroid depth even shallower than the explosion, appears to be even more efficient generating Rg waves that scatter into 1-Hz Lg observed in the far-field. Another key observation is that effects of Rg-to-P scattering are absent in the spectra of Pg waves from underground explosions (Patton and Taylor, 1995), suggesting that this mechanism plays a lesser role in the excitation of regional P waves.

Based on this evidence, I argue that differences in scaling rates of Pn and Lg waves might be caused by the fact that effective source functions for these phases are not similar, nor do they scale alike. The model I will develop is illustrated in the figure below.
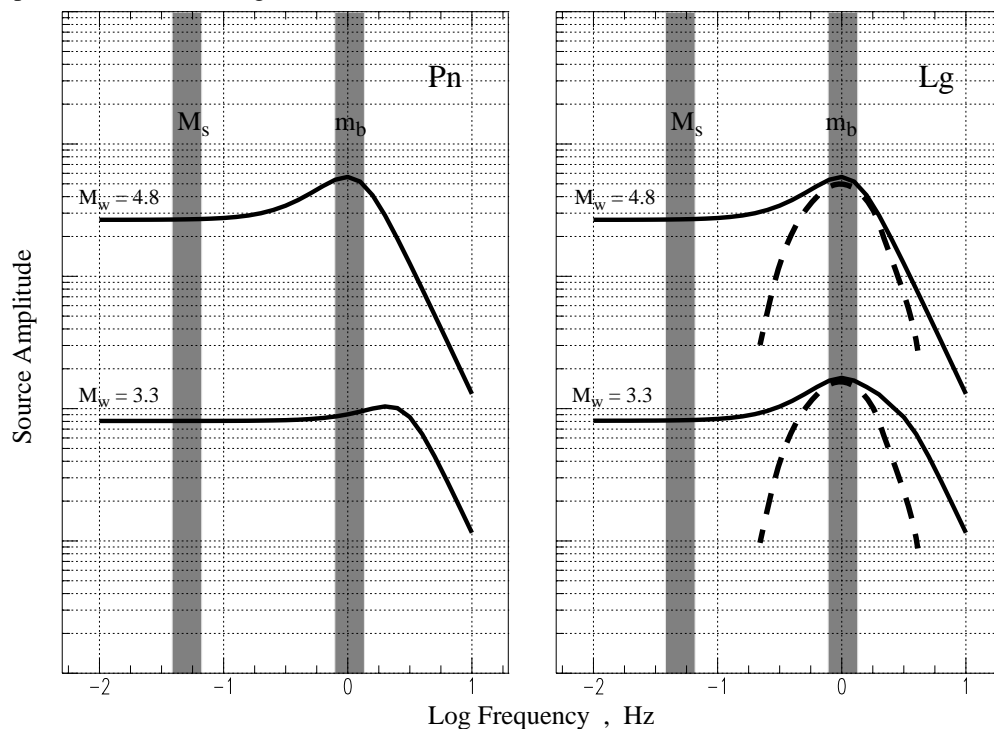

Figure 2. Effective Pn and Lg source functions for explosions with yields of 100 and 1 kt (solid lines) and idealized Rg-to-S scattering functions (dash lines). For illustration purposes, the Lg source function at 100 kt is simply the M-M spectrum plotted for Pn waves, while for 1 kt, it is a hybrid formed by vertically shifting the 100-kt spectrum down, interpolating, and suturing the 1-kt M-M spectrum at ~3 Hz.

The Pn source functions are represented by M-M spectra for 100 and 1 kt explosions in granite with P-wave speeds, α, of 5 km/s, S-wave speeds, β, of 3 km/s, and density, ρ, 2.5 g/cm^3. As source size decreases, the spectral overshoot moves out of the 1-Hz band to higher frequencies. Lg effective source functions are modeled as a composite of the M-M spectrum and a narrow band spectrum representing the contribution of Rg-to-S scattering. While the M-M spectrum scales with source size, the scattering spectrum does not because it is a property of the near-source velocity medium. The bump in Lg spectra is hypothesized to persist at small yields for frequencies near 1 Hz, because Rg-to-S scattering is strong in this band for large and small events.

To relate this model to observations of scaling differences, an analytical expression is needed for the slope, $\Delta m_b(Pn)/\Delta M_w$. First note that

$$M_w \sim 2/3 \cdot \log M_o \sim 2 \cdot (\log \Psi_\infty + \log I_\alpha) / 3 \quad ,$$

and

$$\Delta M_w = 2 \cdot (\Delta \log \Psi_\infty + \Delta \log I_\alpha) / 3 \quad \text{and} \quad I_\alpha = \rho \alpha^2 \quad ,$$

where M_o is the seismic moment of an explosion, which equals $4\pi I_\alpha \Psi_\infty$ (Aki *et al.*, 1974), and Ψ_∞ is the static level of the reduced displacement potential (RDP). I_α is referred to as source medium "impedance." Second, using equation 4.88 of Aki and Richards (1980), we can relate the far-field amplitude, A(f), to the source function, S(f), as follows

$$m_b(Pn) \sim \log A(1\ Hz) \sim \log S(1) - 1/2 \cdot \log \alpha I_\alpha \quad ,$$

and

$$\Delta m_b(Pn) = \Delta \log S(1) - 1/2 \cdot \Delta \log \alpha I_\alpha \quad ,$$

where Pn propagates as a body wave in the mantle and S(1) refers to the source amplitude in the 1-Hz band. Therefore, an analytical expression for the scaling rate of Pn waves is

$$\Delta m_b(Pn)/\Delta M_w = 3/2 \cdot \frac{\Delta \log S(1) - 1/2 \cdot \Delta \log \alpha I_\alpha}{\Delta \log \Psi_\infty + \Delta \log I_\alpha} \quad . \tag{1}$$

Invoking the Mueller and Murphy source model and letting A be Ψ_∞ for a 1-kt explosion, then $AW^{0.76}$ is Ψ_∞ for a W-kt explosion. If B is amplitude of the source function in the 1-Hz band for a 1-kt explosion, then $BKW^{0.76}$ is the amplitude for a W-kt explosion, where K is a measure of overshoot in the source function. Thus, in the range of 1 to W kt, the scaling rate can be written in terms of overshoot parameter K and yield W,

$$\Delta m_b(Pn)/\Delta M_w = 3/2 \cdot \frac{\log K + 0.76 \cdot \log W - 1/2 \cdot \Delta \log \alpha I_\alpha}{0.76 \cdot \log W + \Delta \log I_\alpha} \quad , \tag{2}$$

where $\Delta \log I_\alpha$ is the logarithm of impedance ratio, $I_\alpha{}^W/I_\alpha{}^1$, and superscripts refer to explosion yields.

A similar development is followed to derive an expression for $\Delta m_b(Lg)/\Delta M_w$, except the source is a composite of the explosion and Rg-to-S scattering. Equation (1) above is assumed to apply to Lg waves also, and the scaling of Ψ_∞ obeys the M-M model, just as it does for Pn waves. The development departs from that of Pn waves for the 1-Hz band, where B' is amplitude of the explosion source function, and Φ is amplitude from Rg-to-S scattering. Patton (1990) found that the strength of the spall source (which is proportional to the mass of spalled material) scales as $W^{0.75}$, very nearly the same scaling as Ψ_∞ of the explosion. It follows then that amplitudes for the composite source are $B' + \Phi$ for a 1-kt explosion and $[KB' + \Phi]W^{0.76}$ for a W-kt explosion, assuming linear superposition of the explosion and Rg-to-S sources. The scaling rate for Lg waves can be written in terms of W, K and a new parameter, K',

$$\Delta m_b(Lg)/\Delta M_w = 3/2 \cdot \frac{\log (K+K'-1)/K' + 0.76 \cdot \log W - 1/2 \cdot \Delta \log \alpha I_\alpha}{0.76 \cdot \log W + \Delta \log I_\alpha} \quad , \tag{3}$$

where $K' = 1 + \Phi / B'$. For $K' \geq 2$, the source amplitude due to scattering is as large as or larger than the amplitude of the explosion source function. In the following sub-section, I calculate the range of acceptable models as a function of the material parameter I_α under the constraints imposed by measured scaling rates for Pn and Lg waves and associated uncertainties.

Solution Subspace. Figure 3 shows solutions for K and K′ in the subspace where the central value of $\Delta m_b(Pn)/\Delta M_w$, 1.37, is assumed. Acceptable solutions are bounded by 2-σ errors on the estimate of Lg scaling slope. The plot spans reasonable values for the overshoot parameter K, based on realizations of M-M source functions for media at NTS and yields of ~100 kt. Notice that many solutions give K′ > 2, indicating Lg source amplitudes from Rg-to-S scattering are larger than source amplitudes from the explosion. However, many solutions have unrealistically large K′ values, especially for smaller impedance ratios, where solution space shows rapid increases of K′ values. In order to constrain solution space further, knowledge of an appropriate range for the source impedance ratio is needed for NTS. This is readily available from a large measurement data base that was developed and maintained by weapon laboratories for nuclear test containment studies.
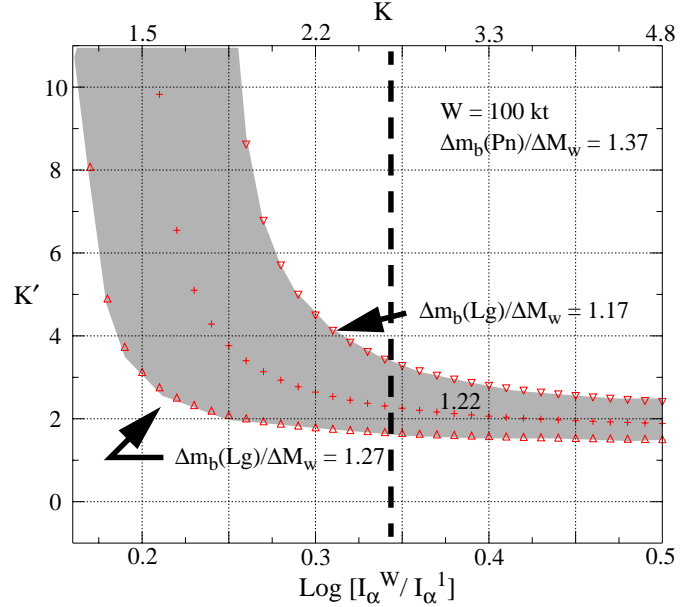

Figure 3. Acceptable solutions (or source models) are located in the shaded region. The central value on Lg scaling rate, 1.22, is the locus of points shown by plus symbols.

Rather than using *in-situ* measurements of working point densities and P-wave speeds, I chose to compute source impedance with a method that gives a better measure of what seismic waves "feel" in the source region. Details were presented in a poster at the 22nd Annual Seismic Research Symposium 12-15 September 2000, but the basic approach is to use measurements of seismic moment M_o and cavity radii (from the containment data base), and calculate "far-field" estimates of I_α using Aki *et al*'s famous equation, $M_o = 4\pi I_\alpha \Psi_\infty$. The results show relationships for I_α between explosions conducted in different media that are expected (e.g. estimates of I_α for dry alluvium are much smaller than for wet tuff). An estimate of I_α^1 was found by taking an average of all data for W < 5 kt, and an estimate of I_α^W was found by taking an average of all data for 50 < W < 200 kt. The log ratio, I_α^W/I_α^1, is 0.34, which is plotted as a vertical dash line in Figure 3. This result is probably a reasonable estimate for M_w-m_b observations used to determine scaling rates of Pn and Lg waves.

For log impedance ratios near 0.35, solution space does not show large variations in K′ as the solution curves are generally flat. Values of K′ are quite reasonable, and the majority of solutions have K′ > 2. This is consistent with the hypothesis that Rg-to-S scattering is an important mechanism for generating 1-Hz Lg waves from underground nuclear explosions. Under this hypothesis, differences in Pn and Lg scaling rates are caused by effective source functions with dis-similar shapes and scaling behavior. The composite source gives a shallower slope because the bump in Lg spectra from Rg-to-S scattering persists for small yields, while it scales out of the 1-Hz band with decreasing yield in the M-M model used for Pn waves.

Implications for m_b-M_s Discrimination. The teleseismic m_b-M_s discriminant is very effective, and its physical basis is well understood (e.g. Stevens and Day, 1985). There is much interest to extend the discriminant to regional-distance applications for monitoring smaller events than teleseismic data can record. The physical

model proposed in this paper builds on our understanding of the explosion source and regional phase excitation. It provides a basis for predicting regional m_b scaling at small magnitudes. Based on the results for NTS, there is reason to believe that, unlike the teleseismic m_b-M_s, the best regional discriminant might be one which utilizes amplitudes of shear-wave phases, such as Lg, for the m_b, not compressional phases.

This project is in the early stages developing data sets to test m_b-M_s scaling predictions at small magnitudes. Part of this work involves developing technologies and calibrating regions for regional M_s determinations; efforts at universities and the lab are well underway for western China and surrounding areas. Plots of regional m_b-M_s for Pn and Lg waves are shown below (Figure 4) as examples of some preliminary data sets I have compiled.
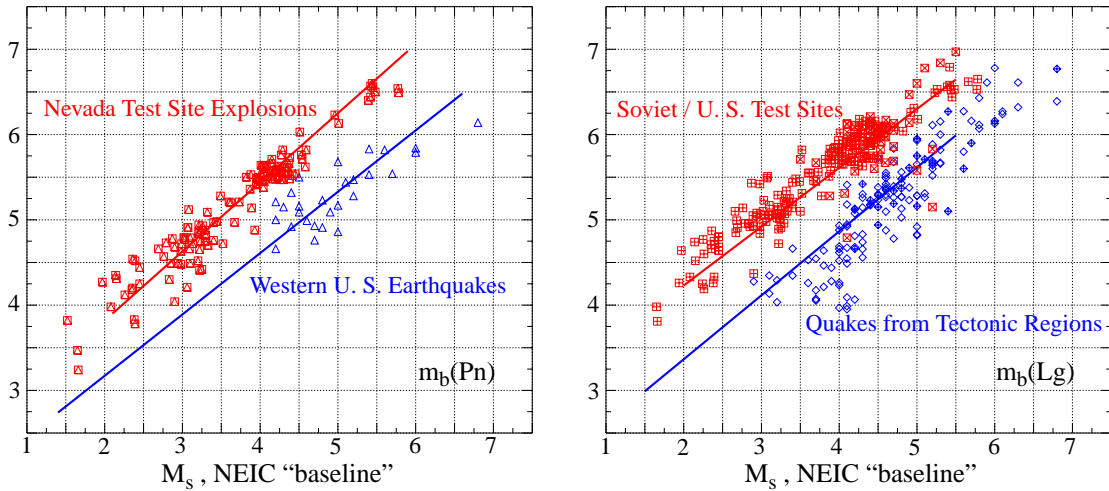

Figure 4. Plots of regional m_b versus M_s for areas in western U. S. and Eurasia. Pn data are just from the western U. S., while transportability of Nuttli's m_b(Lg) enables data from both areas to be plotted on the same graph (Patton, 2000). Measurements of M_s include regional and teleseismic data, and are reduced to a common baseline. Solid lines for earthquake and explosion populations are predictions from M_w versus m_b scaling models.

I have exploited the intrinsic transportability of Nuttli's m_b(Lg) to plot explosion data from NTS, Semipalatinsk, and Novaya Zemlya and earthquake data from tectonic regions of North America and southern Eurasia on a single graph. This is not possible with m_b(Pn) because it has been tied to teleseismic m_b(P) on a region by region basis, and it is well known that m_b(P) shows significant variations worldwide due to regional bias. The results to date are very preliminary, but there is some indication that source populations are better separated at small magnitudes for Lg than they are for Pn, consistent with the scaling models.

CONCLUSIONS AND RECOMMENDATIONS

A major conclusion to date is that m_b(Pn) and m_b(Lg) based on 1-Hz amplitudes show significantly different scaling rates for NTS explosions. This is supported by the analysis of large numbers of regional m_b observations with respect to (1) yield scaling, (2) M_o scaling, and (3) relative scaling of the respective magnitudes over a wide range of source size. A physical model which explains different scaling rates draws on the hypothesis that effective source functions for Lg waves are a composite of two sources, the explosion and near-source Rg-to-S scattering, while Pn waves are generated only by the explosion. Consequently, the shape and scaling behavior of effective source functions for Pn and Lg waves are dis-similar. In light of the evidence that earthquakes do not show differences in scaling rates, I argue that regional m_b-M_s discrimination may perform better for m_b based on shear-waves (Lg) in contrast to traditional compressional-wave based m_b.

A key question is whether or not P-wave scaling differs from Lg at other test sites around the world, especially

those with hard rock. At this point, it is difficult to say because the existing data are limited in quantity and range of source size. This question is important to resolve because it will address issues about the variability of regional m_b-M_s performance and further test our understanding of its physical basis. The latest evidence I have on this score is presented in the poster at the 22nd Annual Seismic Research Symposium.

This is report no. LA-UR-00-3437 of the Los Alamos National Laboratory, Los Alamos, NM 87545.

REFERENCES

Aki, K. and P. Richards (1980), *Quantitative Seismology: Theory and Methods*. W. H. Freeman and Company, San Francisco, CA.

Aki, K., M. Bouchon, and P. Reasenberg (1974), Seismic source function for an underground nuclear explosion. *Bull. Seismol. Soc. Am.* 64, 131-148.

Gupta, I. N., W. Chan and R. Wagner (1992), A comparison of regional phases from underground nuclear explosions at East Kazakh and Nevada Test Sites. *Bull. Seismol. Soc. Am.* 82, 352-382.

Gupta, I. N., T. Zhang, and R. Wagner (1997), Low-frequency Lg from NTS and Kazakh nuclear explosions-- Observations and interpretations. *Bull. Seismol. Soc. Am.* 87, 1115-1125.

Jih, R.-S. (1993), Statistical characterization of rugged propagation paths with application to Rg scattering study. Report No. TGAL-93-06, Teledyne Geotech, Alexandria, VA.

Jih, R.-S. (1995), Numerical investigation of relative contributions of Rg scattering and incomplete dissipation to Lg excitation, in *Proceedings of the 17th Annual Seismic Research Symposium*, James F. Lewkowicz, Jeanne M. McPhetres, and Delaine T. Reiter, editors, Phillips Laboratory Report No. PL-TR-95-2108.

Mueller, R. and J. Murphy (1971), Seismic characteristics of underground nuclear detonations, Part 1: Seismic spectrum scaling. *Bull. Seismol. Soc. Am.* 61, 1675-1692.

Myers, S., W. Walter, K. Mayeda and L. Glenn (1999), Observations in support of Rg scattering as a source for explosion S waves: Regional and local recordings of the 1997 Kazakhstan depth of burial experiment. *Bull. Seismol. Soc. Am.* 89, 544-549.

Nuttli, O. (1986), Yield estimates of Nevada Test Site explosions obtained from seismic Lg waves. *J. Geophys. Res.* 91, 2137-2151.

Patton, H. (1988), Application of Nuttli's method to estimate yield of Nevada Test Site explosions recorded on Lawrence Livermore National Laboratory's digital seismic system. *Bull. Seismol. Soc. Am.* 78, 1759-1772.

Patton, H. (1990), Characterization of spall from observed strong ground motions on Pahute Mesa. *Bull. Seismol. Soc. Am.* 80, 1326-1345.

Patton, H. (2000), Regional magnitude scaling, transportability, and M_s : m_b discrimination at small magnitudes. accepted for publication in *Pure Appl. Geophys.*, special volume on *Monitoring the Comprehensive Nuclear-Test-Ban Treaty.*

Patton, H. and S. Taylor (1995), Analysis of Lg spectral ratios from NTS explosions: Implications for the source mechanisms of spall and the generation of Lg waves. *Bull. Seismol. Soc. Am.* 85, 220-236.

Stevens, J. and S. Day (1985), The physical basis of m_b : M_s and variable frequency magnitude methods for earthquake/explosion discrimination. *J. Geophys. Res.* 90, 3009-3020.

Vergino, E. and R. Mensing (1990), Yield estimation using regional m_b(Pn). *Bull. Seismol. Soc. Am.* 80, 656-674.